

Operational experience with ALICE ITS

L. Barioglio* on behalf of the ALICE Collaboration

University and INFN of Torino

E-mail: luca.barioglio@cern.ch

ALICE (A Large Ion Collider Experiment) is a general purpose heavy-ion experiment designed for the study of strongly-interacting matter at the extreme energy densities that characterise Pb-Pb collisions at the CERN LHC, where the formation of the Quark-Gluon Plasma (QGP), a deconfined phase of matter, is expected. The innermost detector of ALICE is the Inner Tracking System (ITS). The ITS consists of six cylindrical layers of silicon detectors based on different technologies: two inner layers with pixel sensors (Silicon Pixel Detector), two intermediate layers with drift sensors (Silicon Drift Detector), two outer layers with strip sensors (Silicon Strip Detector). The ITS is used for the reconstruction of primary and secondary vertices, for particle tracking, for a precise determination of the impact parameter and for particle identification at low momentum. In this report, after a brief description of the three sub-detectors, the operational experience with the ITS during LHC Run2 is summarised, describing the status and the performance of the detector.

*The 27th International Workshop on Vertex Detectors - VERTEX2018
22-26 October 2018
MGM Beach Resorts, Muttukadu, Chennai, India*

*Speaker.

1. Introduction

ALICE (A Large Ion Collider Experiment)[1] is designed for the study of strongly-interacting matter and in particular of the properties of the Quark-Gluon Plasma, a deconfined phase of matter produced in extreme energy-density conditions, such as in ultra-relativistic heavy-ion collisions. Besides Pb-Pb collisions, the ALICE experimental program includes also pp and p-Pb collisions, which are needed as reference for the study of the underlying collision dynamics.

The experimental apparatus can be divided into two different pseudo-rapidity regions. The forward muon arm covers the forward pseudo-rapidity region $-4.0 < \eta < -2.5$ and is used to measure heavy-flavoured hadrons, quarkonia and light vector mesons. The central barrel covers the pseudo-rapidity region $|\eta| < 0.9$ and the full azimuthal angle. The detectors in the central barrel are embedded in a solenoidal magnet, which provides a magnetic field up to 0.5 T. The two main tracking detectors in the central barrel are the Inner Tracking System (ITS) [2] and the Time Projection Chamber (TPC) [3]. The low material budget of the ITS and of the TPC ($\sim 10\% X_0$) allows the reconstruction of charged-particle trajectories in a wide transverse momentum range (0.1 - 100 GeV/c). Moreover, the central-barrel detectors allow the particle identification (PID) up to 20 GeV/c through the measurement of the specific energy loss dE/dx in the ITS and in the TPC and of the time of flight in the dedicated detector, with a resolution of 60 ps in Pb-Pb collisions.

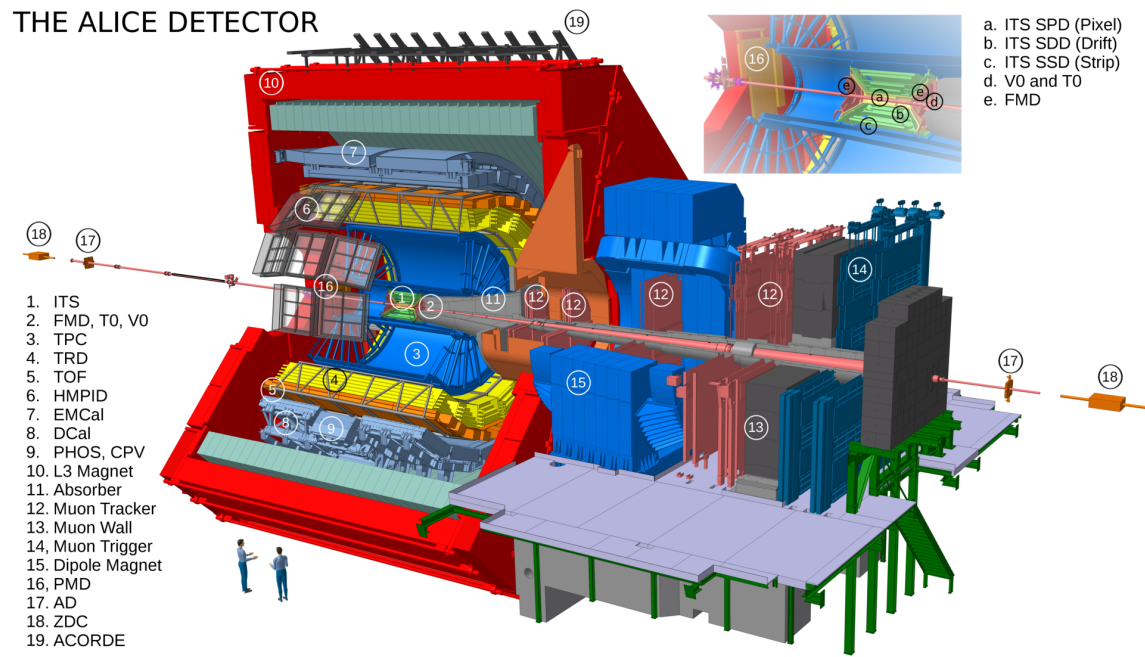


Figure 1: Schematic of the ALICE apparatus. A zoom of the ITS is show on the top-right corner.

2. The Inner Tracking System

The Inner Tracking System is the closest detector to the interaction point and has several purposes. The ITS is used for the reconstruction of the collision point (primary vertex), with a resolution of $10 \mu\text{m}$ in central Pb-Pb collisions, and the displaced vertices (secondary vertices), with a resolution better than $100 \mu\text{m}$. The precision of the reconstruction of the primary vertex, together with the possibility to measure the impact parameter, i.e. the distance of closest approach of a track to the vertex, with a resolution of $\sim 60 \mu\text{m}$ at $p_T = 1 \text{ GeV}/c$, makes it possible to study particles characterised by a short decay length, such as open heavy-flavoured hadrons. The ITS allows the reconstruction of the trajectories down to $0.1 \text{ GeV}/c$. Finally, the ITS can be used for PID at low transverse momentum via the measurement of the specific energy loss dE/dx in the four outermost layers of the detector. In particular, it is possible to separate kaons from pions in the ranges of $(0.1 - 0.45) \text{ GeV}/c$ and kaons from protons in the range of $(0.1 - 1) \text{ GeV}/c$ (Figure 2). The ITS consists of six cylindrical layers of silicon detectors based on different technologies. A representation of the ITS within the ALICE experimental apparatus is shown in Fig. 1 and the characteristics of the ITS and its sub-detectors can be seen in Table 1.

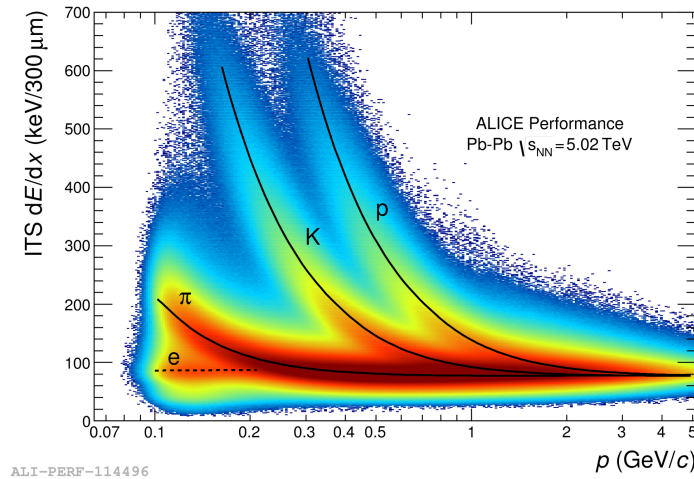


Figure 2: ITS specific energy loss as a function of momentum in Pb-Pb collisions at $\sqrt{s_{NN}} = 5.02 \text{ TeV}$.

2.1 The Silicon Pixel Detector (SPD)

The two innermost layers form the Silicon Pixel Detector (SPD). It consists of 120 Half-Stave modules, grouped in two Half-Barrels. Each Half-Barrel contains 10 Half-Sectors, containing six Half-Staves, two from the first layer and four from the second. The Half-Stave is composed of two ladders, which contain one sensor and five readout chips each. The sensor is a matrix with 256×160 reversed biased (50 V) p^+n diodes, forming pixels with size $50 \mu\text{m} \times 425 \mu\text{m}$. The sensor is $100 \mu\text{m}$ thick and it is connected via bump-bonding to the five $200 \mu\text{m}$ thick readout chips. The sensors are characterised by a binary readout, therefore the SPD is not suitable for PID. The detector is equipped with a C_4F_{10} evaporative cooling system. The SPD is also used as first-level trigger. Not only it can be used as a multiplicity related trigger, based on the number

Layer	Detector	Radius	Length	Channels	Area	Res. (μm)		M.B.
		(cm)	(cm)		(m^2)	$r\phi$	z	(% X_0)
1	SPD	3.9	28.2	3.3 M	0.07	12	100	1.14
2		7.6	28.2	6.5 M	0.14			1.14
3	SDD	15.0	44.4	43 k	0.42	35	25	1.13
4		23.9	59.4	90 k	0.89			1.26
5	SSD	38.0	86.2	1.1 M	2.20	20	830	0.83
6		43.0	97.8	1.5 M	2.80			0.83

Table 1: Characteristics of the ITS, layer by layer. *Res.* is the resolution, along the bending direction ($r\phi$) and the beam axis (z). *M.B.* is the material budget, expressed in terms of radiation lengths (X_0).

of SPD tracklets, i.e. the segment obtained coupling pairs of points on the two layers, but also as topological trigger. Indeed, when used as double-gap diffractive trigger, two conical regions in the acceptance are selected and the angle between the two cones, as well as the number of tracklets in each region, can be varied.

2.2 The Silicon Drift Detector (SDD)

The Silicon Drift Detector (SDD) forms the two intermediate layers of the ITS. It consists of 260 modules. A module is composed of a $300 \mu\text{m}$ thick drift sensor and two hybrid boards with the readout electronics. A scheme of the drift sensor is shown in Fig. 3. It is divided into two drift regions along the bending direction (orthogonal to the beam line), separated by a high voltage cathode at -1.8 kV . The cathode potential generates a uniform electric drift field, parallel to the surface, directed towards the 512 collection anodes. The cathodes have a pitch of $294 \mu\text{m}$ and are located at the edges of the sensor. The drift speed is about $6.7 \mu\text{m/s}$ and is monitored with MOS charge injectors. Indeed, in each drift regions three lines of MOS injectors are present: one is close to the cathode, another is in the middle of the drift region, the last is close to the cathodes. The drift speed is measured in specific calibration runs at the beginning of each LHC fill. The SDD is provided with a leak-less water cooling system. Finally, the SDD is also used to perform PID through the measurement of the charge collected at the anodes and consequently of the specific energy loss.

2.3 The Silicon Strip Detector (SSD)

The two outermost layers of the ITS constitute the Silicon Strip Detector (SSD). It consists of 1698 modules and each module is composed of 768 double-sided strip sensors, with a thickness of $300 \mu\text{m}$, connected with 12 front-end chips. The p and n strips have a pitch of $95 \mu\text{m}$ (along the bending direction), a length of 40 mm and their inclination angle is respectively of 7.5 mrad and 27.5 mrad with respect to the beam axis. The SSD shares with the SDD the leak-less water cooling system. However, due to the sensitivity of the detector to the air humidity an air drier system is

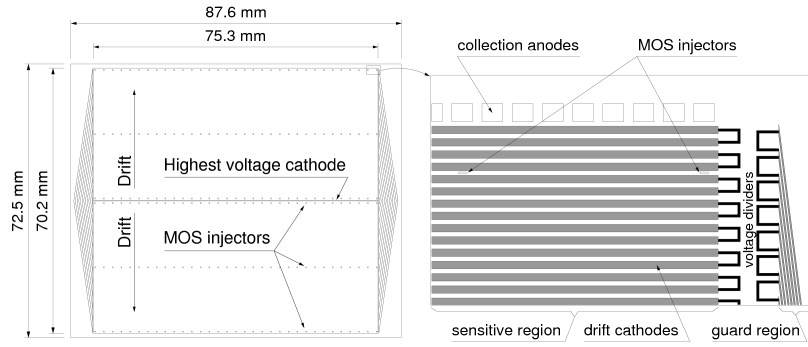


Figure 3: Scheme of the drift sensor of the SDD.

used to keep the absolute humidity between 1 and 1.5 g/kgas. Finally, thanks to the analogical readout, it is possible to perform the PID measuring the charge collected by the anodes.

3. The ITS performance

	Availability (%)			Acceptance (%)		
	SPD	SDD	SSD	SPD	SDD	SSD
Run1 (2013)	96.0	92.0	96	92	87	91
Run2 (2015-2016)	99.6	98.4	98.6	93	83	91
Run2 (2017)	99.9	99.5	100.0	93	82	91
Run2 (2018)	99.6	99.8	99.8	92	81	91

Table 2: Availability and acceptance of the three ITS sub-detectors during Run1 and Run2, expressed in terms of fraction of data acquisition-time and number of modules respectively.

The ITS operational efficiency is summarised in Table 2, which reports the availability of the ITS sub-detectors, expressed in terms of the fraction of the data-acquisition time, and the acceptance, as the number of modules in acquisition. Generally, for all the detectors the availability was stable during Run2 and improved with respect to Run1. The improvement was possible thanks to the firmware update of the readout electronics, to the automation of recovery procedures and as a result of the interventions that took place during Run1 and the following Long Shutdown (LS1).

The main intervention involved the SPD. In 2011 only 63% of the SPD could be powered on, due to an insufficient flow of the liquid freon in the cooling system. The reason was that some of the filters in the cooling line were clogged by metal and graphite fragments. However, the operation of unclogging was not trivial, since the clogged filters were located in an inaccessible position. The adopted solution consisted in drilling the clogged filters to restore the nominal flow and installing new filters upstream, close to the pump [4]. A dedicated tool constituted by a tungsten carbide tip welded on a stainless steel wire (5 m long and 2.5 mm thick) was used. The drilling campaign took

place from February 2012 to January 2014, bringing the number of modules in acceptance from 63% to 92% at the end of Run1.

Concerning the SDD, the most recurring problems during Run1 were the loss of communication of one module and the presence of an error in the Common Data Header (CDH), interpreted as a consequence of a Single Event Upset (SEU) event. The recovery time necessary to reset the configuration of the front-end electronics was reduced in the transition between Run1 and Run2, improving the availability of the detector. The SDD readout boards were replaced with new ones, the SuperCARLOSrx, equipped with a more powerful Field Programmable Gate Array (FPGA). With the new boards it was possible to design a new firmware and hence obtain a better data compression and, above all, to reduce the recovery time to $800 \mu s$. As a result the configuration of the electronics could be reset without stopping the data acquisition. The number of modules in acquisition was lower than the other sub-detectors because of many losses suffered during Run1. For example, during the installation of the detector a half-ladder in the third layer lost communication with the readout electronics and it was not possible to recover it, due to the inaccessibility of the ITS and the consequent impossibility to replace modules. Then, during a beam dump that occurred close to ALICE, the third layer suffered from high radiation exposure, that caused the loss of many MOS injectors. Since then, as precaution, both HV and LV power suppliers are turned off during beam operations.

One of the most recurrent problem with the SSD was caused by a SEU event affecting the read-out electronics, in particular with the SRAM FPGA of the Front End Read Out Modules (FEROM). The FEROMs are located in the cavern, close to the magnet but sheltered by a concrete shield. For this reason SEUs were not expected. In Fig. 4 the integrated number of SEUs since 2015 is shown, together with the integrated fluence of High Energy Hadrons (HEH), measured with a sensor within the FEROM crate. The correlation between the number of SEU events and the integrated dose is straightforward. After Run1 some countermeasures were adopted. In particular, the PROMs in the FEROMs were replaced with new radiation tolerant PROMs and the FPGA firmware was updated, reducing the recovery time from 20 minutes to 5 minutes.

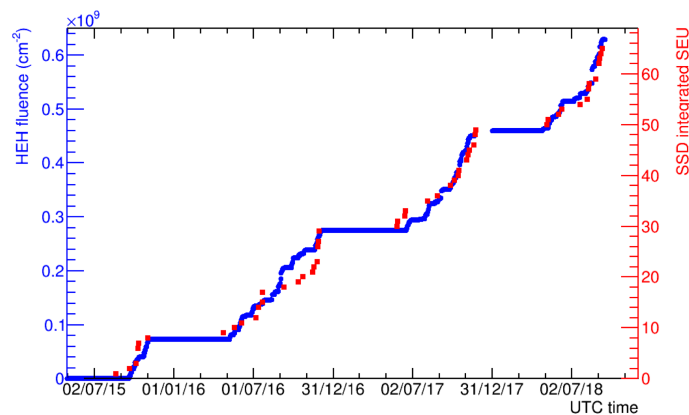


Figure 4: Integrated number of SEU events and integrated HEH fluence since 2015.

4. Summary and conclusions

In Run1 and Run2 the ITS worked with high efficiency, providing a performance in agreement with the design requirements. During the data acquisition some unexpected problems showed up, such as the clogged filters of the SPD cooling system, the effects of SEU events and other issues related to the readout electronics. However, these accidents gave the opportunity to get a better understanding of the detector and finally were solved, increasing the efficiency of the data acquisition. The Long Shutdown 2 started in January 2019 and the current ITS will be completely replaced by a new tracker. The ITS-Upgrade [5] will be equipped with seven layers of monolithic silicon pixel sensors. The improved tracking and readout capabilities of the ITSU will allow to extend the physics reach of ALICE concerning heavy-flavours and rare probes.

References

- [1] ALICE collaboration, *The ALICE experiment at the CERN LHC*, *JINST* **3** (2008) S08002.
- [2] ALICE COLLABORATION collaboration, *ALICE Inner Tracking System (ITS): Technical Design Report*, Technical Design Report ALICE. CERN, Geneva, 1999.
- [3] ALICE collaboration, *ALICE: Technical design report of the time projection chamber*, .
- [4] D. Colella, *Alice its: the run 1 to run 2 transition and recent operational experience*, *PoS* (2015) 003.
- [5] A. Collaboration, B. Chang, D. J. Kim, J. Kral, A. Morreale, J. Rak et al., *Technical design report for the upgrade of the alice inner tracking system*, *Journal of Physics G: Nuclear and Particle Physics* **41** (2014) .